THE FASEB JOURNAL • RESEARCH • www.fasebj.org

Novel imaging of the prostate reveals spontaneous gland contraction and excretory duct quiescence together with different drug effects

Robert Kügler,[*,1] Andrea Mietens,[*,1] Mathias Seidensticker,[*,1] Sabine Tasch,[*] Florian M. Wagenlehner,[†] Andre Kaschtanow,[*] Yudy Tjahjono,[*] Claudia U. Tomczyk,[*] Daniela Beyer,[*] Gail P. Risbridger,[‡] Betty Exintaris,[§] Stuart J. Ellem,[‡] and Ralf Middendorff[*,2]

[*]Institute of Anatomy and Cell Biology and [†]Department of Urology, Pediatric Urology, and Andrology, Justus-Liebig-University Giessen, Giessen, Germany; [‡]Department of Anatomy and Developmental Biology, Monash University, Melbourne, Victoria, Australia; and [§]Drug Discovery Biology, Monash Institute of Pharmaceutical Sciences, Melbourne, Victoria, Australia

ABSTRACT: Prostate carcinoma and benign prostate hyperplasia (BPH) with associated lower urinary tract symptoms (LUTS) are among the most prevalent and clinically relevant diseases in men. BPH is characterized by an enlargement of prostate tissue associated with increased tone of smooth muscle cells (SMCs) which surround the single glands composing the prostate. Secretions of the glands leave the prostate through local excretory ducts during the emission phase of ejaculation. Pharmacological treatment of BPH suggests different local drug targets based on reduction of prostate smooth muscle tone as the main effect and disturbed ejaculation as a common side effect. This highlights the need for detailed investigation of single prostate glands and ducts. We combined structural and functional imaging techniques—notably, clear lipid-exchanged, acrylamide-hybridized rigid imaging/immunostaining/*in situ* hybridization–compatible tissue-hydrogel (CLARITY) and time-lapse imaging—and defined glands and ducts as distinct SMC compartments in human and rat prostate tissue. The single glands of the prostate (comprising the secretory part) are characterized by spontaneous contractions mediated by the surrounding SMCs, whereas the ducts (excretory part) are quiescent. In both SMC compartments, phosphodiesterase (PDE)-5 is expressed. PDE5 inhibitors have recently emerged as alternative treatment options for BPH. We directly visualized that the PDE5 inhibitors sildenafil and tadalafil act by reducing spontaneous contractility of the glands, thereby reducing the muscle tone of the organ. In contrast, the ductal (excretory) system and thus the prostate's contribution to ejaculation is unaffected by PDE5 inhibitors. Our differentiated imaging approach reveals new details about prostate function and local drug actions and thus may support clinical management of BPH.—Kügler, R., Mietens, A., Seidensticker, M., Tasch, S., Wagenlehner, F. M., Kaschtanow, A., Tjahjono, Y., Tomczyk, C. U., Beyer, D., Risbridger, G. P., Exintaris, B., Ellem, S. J., Middendorff, R. Novel imaging of the prostate reveals spontaneous gland contraction and excretory duct quiescence together with different drug effects. FASEB J. 32, 1130–1138 (2018). www.fasebj.org

KEY WORDS: contractility · time-lapse imaging · 3D imaging · PDE5 inhibitors

Benign prostatic hyperplasia (BPH) is a highly prevalent, nonmalignant disease that affects aging men and results in serious lower urinary tract symptoms (LUTS) (1). Morphologically, BPH is mainly characterized by an increase in interstitial stroma, leading to an increase in prostate size. In the human prostate, smooth muscle cells (SMCs) are an important component of the interstitial stroma among the glands. Blood vessels and the prostate excretory ducts are additional prostate structures that are characterized by copious amounts of SMCs (2–4). The ducts function to transport secretions from individual glands of the prostate, which are responsible for one-third of the ejaculate (5), toward the urethra and are of particular importance for the emission phase of ejaculation.

Most of the drugs used for the treatment of LUTS and BPH target SMC function (6). α_1-Adrenergic blockers (*e.g.*, tamsulosin and silodosin) are well-established drugs for BPH treatment (7, 8), but are associated with significant

ABBREVIATIONS: BPH, benign prostatic hyperplasia; CLARITY, clear lipid-exchanged acrylamide-hybridized rigid imaging/immunostaining/*in situ* hybridization-compatible tissue-hydrogel; LUTS, lower urinary tract symptoms; PDE, phosphodiesterase; SMA, α-smooth muscle actin; SMC, smooth muscle cell

[1] These authors contributed equally to this work.

[2] Correspondence: Institute of Anatomy and Cell Biology, Justus-Liebig-University Giessen, Aulweg 123, D-35392 Giessen, Germany. E-mail: ralf.middendorff@anatomie.med.uni-giessen.de

doi: 10.1096/fj.201700430R
This article includes supplemental data. Please visit *http://www.fasebj.org* to obtain this information.

0892-6638/18/0032-1130 © FASEB

side effects such as ejaculation disorders (9–11). Phosphodiesterase (PDE)-5 inhibitors (*e.g.*, tadalafil) are promising new therapeutic options for the treatment of BPH (12–17). PDE5 hydrolyzes the second messenger cGMP, which is produced by binding of NO and natriuretic peptides to specific guanylyl cyclases (18). PDEs essentially regulate the duration of cGMP action (19). In their most recent review, Gacci *et al.* (20) describe a series of cGMP/PDE5 actions in LUTS and BPH such as modulation of oxygenation, inflammation, proliferation, and nerve activity. However, the most established mechanism of action of PDE5 inhibitors is smooth muscle relaxation leading to reduced muscle tone (20, 21). PDE5 inhibitors have been shown to relax isolated prostate strips in numerous species (14, 21–23).

Information on the spatial arrangement of the SMCs and PDE5-expressing cells in the stromal compartment is scarce, whereas direct visualization and demonstration of the effects of PDE5 inhibition has not been shown. Moreover, knowledge about PDE5 expression in the ducts and their susceptibility to PDE5 inhibitors is completely lacking. These data are of particular importance, especially since a characteristic adverse side effect of other BPH therapeutics, such as α_1-adrenergic blockers, is abnormal and decreased ejaculation (24, 25). In this study, we used novel imaging techniques to examine the effects of PDE5 inhibitors on the different muscular structures of the prostate, including those involved in ejaculation.

MATERIALS AND METHODS

Tissues

Human tissue samples originated from patients (age range, 60–79 yr; median, 71.7 ± 6.5) undergoing transurethral monopolar electroresection of the prostate for BPH or radical prostatectomy for prostate cancer. Use of human prostate tissue was approved by the ethics committee of the Medical Faculty, Justus-Liebig-University Giessen, Germany (ethical vote 49/05, 2005), and all patients gave written informed consent.

Rat prostate tissue was obtained from adult Wistar rats housed in the animal facility of Justus-Liebig-University Giessen. Housing, animal care and all procedures were conducted according to the guidelines for animal care and approved by the committee for laboratory animals of Justus-Liebig-University Giessen (JLU no. 469_M and 510_M).

Tissues were fixed in 4% paraformaldehyde for histologic analyses or immediately processed for further investigation. Rat tissue was carefully dissected under a binocular microscope by using fine surgical scissors to isolate single prostate glands and ducts from the ventral lobes (26).

Time-lapse imaging

Tissue was immobilized for transillumination microscopy by embedding in collagen gel (27) and maintained in Minimal Essential Medium (Thermo Fisher Scientific, Waltham, MA, USA). Frames were captured every 2 s. Sildenafil, tadalafil, and noradrenaline were used at a final concentration of 5, 2.5 and 10 μM, respectively, to ensure diffusion into the tissue. The duration of the treatments was 12–15 min. In all series of experiments (total tissue, glands, and ducts), between 5 and 8 different individual samples from 5 to 8 patients or animals were investigated.

To visualize contractile activity, time-lapse images were treated as a stack of frame shots taken at regular time intervals (time stack). By placing a virtual section through the time stack, a specific region (indicated as a blue bar in the relevant overview pictures) can be followed over time (27). Contractions become visible as twitches or little peaks and were marked by arrows, the contractions were counted and analyzed with ImageJ 1.50e (public domain software; U.S. National Institutes of Health, Bethesda, MD, USA). Contrast enhancement was used if necessary to improve discrimination of twitches. Noradrenaline-induced contraction in prostate ducts was quantified by comparing ductal areas before and after addition of noradrenaline (see Fig. 4*D*). Afterward, the tissue used in the assays was paraffin embedded for azan staining.

Immunostaining

For immunofluorescence staining of paraffin sections we used monoclonal mouse anti-α-smooth muscle actin (SMA,1:1000; Millipore-Sigma, St. Louis, MO, USA), rabbit polyclonal anti-PDE5 (1:1000; generous gift from Laurinda Jaffe, University of Connecticut Health Center, Farmington, CT, USA) and the fluorescence-labeled secondary antibodies Cy3 anti-mouse IgG (1:500; Jackson ImmunoResearch, West Grove, PA, USA) and Alexa Fluor 488 anti-rabbit IgG (1:500; Thermo Fisher Scientific, Waltham, MA, USA).

Clear lipid-exchanged acrylamide-hybridized rigid imaging/immunostaining/*in situ* hybridization-compatible tissue-hydrogel

Clear lipid-exchanged acrylamide-hybridized rigid imaging/immunostaining/*in situ* hybridization-compatible tissue-hydrogel (CLARITY) (28) is a spatial advancement of common histochemical techniques and allows generating a 3-dimensional image of whole tissues. It offers the possibility of transforming intact biologic tissue into a translucent hydrogel-tissue hybrid by removing lipid components responsible for light scattering and thus tissue opacity. In this form, the hybrid is permeable to agents such as specific antibodies, and imaging against a translucent background can be greatly enhanced .

Patient tissue samples and rat tissue of ~1 mm^3 were treated as described by Yang *et al.* (29) with a few modifications (30). Tissue sections were fixed in 4% paraformaldehyde for 24 h at 4°C. Prostate tissue was incubated in hydrogel-forming solution [acrylamide 4% in PBS, bis-acrylamide 0.05% in PBS and 0.25% 2,2′-azobis(2-methylpropionamidine) dihydrochloride] for 24 h at 4°C followed by polymerization at 37°C for 3 h. Tissue sections were cleared in a solution containing SDS 10% and boric acid 200 mM (pH 7.4) in water, for at least 5 d. Extensive washing steps with PBS-Triton 0.1% were performed before and after adding primary antibodies. Primary and secondary antibodies were the same as mentioned above (see immunostaining), but at dilutions of 1:100 and 1:200, respectively. Antibodies were diluted in PBS-Triton 0.1% and incubated for at least 5 d at room temperature. After further washing steps (24 h), tissue was transferred into a refractory index–matching buffer: Histodenz 88% (D2158; Millipore-Sigma) in 0.02 M phosphate buffer with 0.1% Tween-20 and 0.01% sodium azide (pH 7.5) for 24 h at room temperature. Documentation was performed on an LSM 710 Confocal Laser Scanning Microscope (Zeiss, Jena, Germany), *Z*-stacks were captured every 1.5–5 μm and reconstructed in ImageJ by using the command "3D projects," allowing interpolation and contrast autoenhancement if necessary.

Statistical analysis

Only vital samples (confirmed by a visible response to noradrenaline) were included. Normal distribution of the data was checked by the Kolmogorov-Smirnov test. Contraction frequencies were analyzed by paired 1-tailed *t* tests for normally distributed data; otherwise, the Mann-Whitney *U* test was applied. For noradrenaline effects in the ducts, assessed as areas before and after treatment, paired 2-tailed *t* tests were used. All statistical procedures were performed with GraphPad Prism software (version 4.03; GraphPad Software, La Jolla, CA, USA).

RESULTS

All SMC compartments of the prostate show PDE5 expression

Prostate tissue comprises glands and their ducts (**Fig. 1*A, B***) which transport glandular secretions toward the urethra. Both are encompassed by interstitial tissue including also blood vessels (Fig. 1*A*). In the human prostate, SMCs (marked by SMA immunostaining) are found, not only in the interstitial tissue around prostate glands (Fig. 1*C, F*) and in blood vessels (Fig. 1*H*), but also in the ducts (Fig. 1*J, L, M*). Bigger ducts (Fig. 1*J, L*) are distinguished by several SMC layers surrounding the epithelial layer (Fig. 1*J, L, M*). In our efforts to reveal the prostate targets of drugs used for BPH treatment, we localized PDE5, the enzyme affected by PDE5 inhibition. PDE5 immunoreactivity was regularly observed in interstitial SMCs, confirmed by double staining of SMA and PDE5 (Fig. 1*C–E*). CLARITY visualized the 3-dimensional arrangement of PDE5-expressing SMCs thereby providing a better understanding of the spatial architecture of these cells which fill the interstitial compartments and are oriented in various directions (Fig. 1*F, G* and Supplemental Movies 1 and 2). PDE5 is also expressed in vascular SMCs (Fig. 1*H, I*) and in the SMCs of the larger (Fig. 1*J–L*) and smaller (Fig. 1*M*) prostatic ducts.

Relaxing effects of PDE5 inhibition can be directly visualized in human prostate

Time-lapse imaging of human prostate tissue was performed to directly visualize contractions of interstitial SMCs in their regular environment and to monitor effects of PDE5 inhibition. Slow spontaneous contractions of the tissue were readily observed. The PDE5 inhibitor sildenafil markedly reduced spontaneous contractile frequency (**Fig. 2*A*** and Supplemental Movie 3). Further treatment with noradrenaline confirmed functional integrity and viability of the tissue sample. Figure 2*C* gives a visual impression of contractions and sildenafil effects; in this example, sildenafil even abolished spontaneous contractions. Statistical analysis showed that PDE5 inhibition by sildenafil significantly reduced spontaneous contractile frequency (Fig. 2*D*). After time-lapse imaging, histologic evaluation of the tissue showed SMCs oriented in the various directions in the interstitial compartment around glandular tissue (Fig. 2*B*).

Isolated prostate glands show spontaneous contractions that are inhibited by PDE5 inhibition

Our CLARITY approach 3-dimensionally demonstrated that the interstitial periglandular SMCs in rat prostate (**Fig. 3*A*** and Supplemental Movie 4) were arranged tighter around the glands, than in the human prostate, where SMCs were widely dispersed in the interstitium (see Fig. 1*F* and Supplemental Movie 1). This structural difference enabled visualization and analysis of the contractile pattern of single, isolated glands with their musculature. Movies revealed spontaneous contractility occurring in a slightly irregular pattern (Fig. 3*B* and Supplemental Movie 5). Following wall movements through the time stack at the indicated position (Fig. 3*B*), the contractile pattern and the drug effects were analyzed (Fig. 3*C*). Addition of sildenafil resulted in a clearly visible (Fig. 3*B, C* and Supplemental Movie 5) and significant (Fig. 3*D*) reduction of contractile frequency. The response to noradrenaline confirmed viability of the tissue (not displayed). Analogous experiments were performed using the PDE5 inhibitor tadalafil. Our findings showed a reduction of spontaneous contractile frequency in rat prostate glands by tadalafil (Fig. 3*E*), as seen before by sildenafil.

In line with our functional studies PDE5 was found in SMCs surrounding rat prostate glands, as indicated by SMA and PDE5 double staining (Fig. 3*F, G*). Corresponding to the human tissue (Fig. 1) PDE5 was also found in SMCs of blood vessels (Fig. 3*F–K* and Supplemental Movie 6) and prostate ducts (Fig. 3*I–K*). Interestingly, the composition of prostate ducts in rat (Fig. 3*I*) and human (Fig. 1*J*) and their PDE5 expression in surrounding SMCs (Fig. 3*I–K vs.* Fig. 1*J–M*) is comparable.

Prostate ducts do not contract spontaneously. Contractions induced by noradrenaline, mediating emission and ejaculation, are not disturbed by PDE5 inhibition.

Whereas the role of PDE5 inhibitors in vasculature has already been discussed (20), nothing is known about the functional relevance of PDE5 inhibitors in prostate ducts with their large amount of PDE5-expressing SMCs. Therefore, prostate ducts were isolated and investigated by our life-imaging approach *ex vivo* (**Fig. 4*A***). As can be seen in Supplemental Movie 7 and the corresponding time stack analyses (Fig. 4*B*) the duct did not show (spontaneous) contractions without treatment, which contrasts with the regular observation of spontaneous contractility in glands (see Figs. 2 and 3). No obvious sildenafil effect was visible in the duct samples—in particular, no dilatation was seen. Noradrenaline, however, when used to test the viability of the tissue and to mimic sympathetic stimulation of the prostate during ejaculation, resulted in a rapid and strong contraction of the whole duct (Fig. 4*B* and Supplemental Movie 7), also illustrated by a distinct area change (Fig. 4*D*). Spillage of secretions from the duct during the noradrenaline-induced contraction was also noted (Supplemental Movie 7). In contrast, the glands

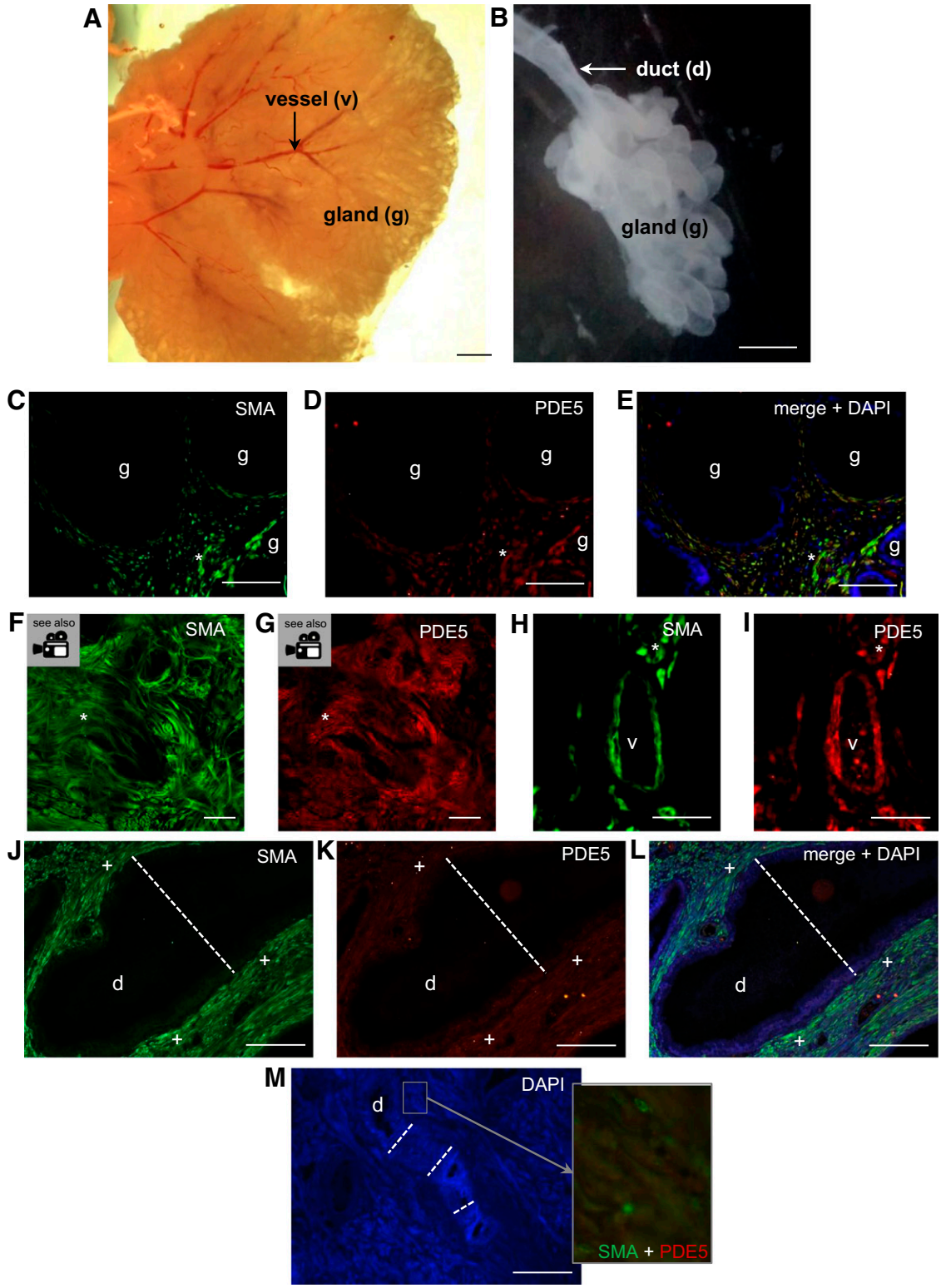

Figure 1. Localization of PDE5 in SMCs of glands, vessels, and ducts of the human prostate. *A*, *B*) Preparation of glandular structures of the prostate showed glands (g) and ducts (d) to be the components of the secretory and transport system in addition to vessels (v) as part of the interstitial tissue. SMC localization of PDE5 in human prostate. *C*–*G*) PDE5 in human interstitial SMCs. In the human prostate, interstitial SMCs were identified by SMA expression in the stromal compartment (*) around the glands (g). PDE5 expression was colocalized to these SMA-positive cells, as shown in the merged image. *E*) DAPI staining helped to identify the location of the epithelium. *F*, *G*) Movie frame shots from double staining of SMA and PDE5 in the human prostate using a 3-dimensional CLARITY approach showed congruent localization of both antigens. Please refer to the corresponding Supplemental Movies 1 and 2 to appreciate the spatial architecture. *H*, *I*) PDE5 in human vascular SMCs. Immunostaining with SMA and PDE5 confirmed an equal distribution in vascular (v) contractile cells in human prostate, stromal interstitial cells are

(*continued on next page*)

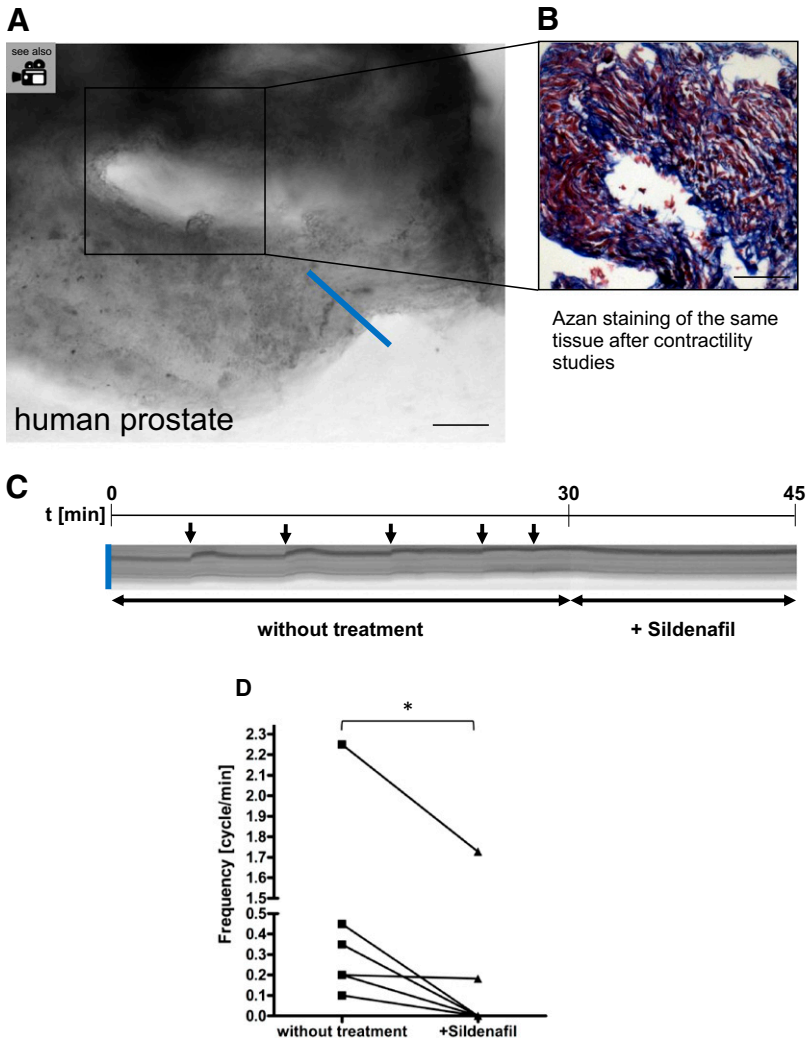

Figure 2. Visualization of spontaneous contractility of human prostate tissue sensitive to PDE5 inhibition. *A*) Frame shot from Supplemental Movie 3 shows a piece of human prostate tissue by transillumination imaging and indicates the location of the virtual slice (blue line) which is followed through the time stack in *C*. Scale bar, 75 μm. *B*) Azan staining of one 6 μm section from the tissue used in (*A*). Interstitial SMCs stained red. Scale bar, 75 μm. *C*) Contractions elicited small movements of the human prostate tissue and became visible as little twitches (marked by vertical arrows for better visibility). Slow, spontaneous, irregular contractions are visible, and their frequency is reduced (or even abolished in this example) after the addition of the PDE5 inhibitor sildenafil. *D*) Statistical analysis of 6 human samples showed a significant reduction of spontaneous contractile frequency by sildenafil. $*P \leq 0.05$.

contracted only slightly, and no relevant area change was visible.

The PDE5 inhibitors used to treat BPH interfered with the prostatic component of ejaculation. We therefore investigated systematically whether (pre)treatment of the prostate duct with sildenafil changes the contractile response to noradrenaline, the key player for the initiation of ejaculation. For this, we cut prostate ducts in two parts (Fig. 4*C*). Each duct served as its own control (Fig. 4*C*) and was exposed to sildenafil (+Sild.) or vehicle (−Sild.). To assess and quantify noradrenaline-induced contractions, we used frame shots from movies before and after the addition of noradrenaline and compared the area occupied by the tissue as a surrogate parameter for the contraction (Fig. 4*D*). To confirm that the samples used in the contraction assay were correctly classified as prostate ducts, we used Azan-stained histologic sections (Fig. 4*E*) and found the typical architecture of prostate ducts consisting of several smooth muscle layers around the epithelium. Noradrenaline-induced contractions of the isolated duct segments occurred irrespective of sildenafil pretreatment and in both cases, the area after noradrenaline treatment was ~80%, compared with the area before treatment (Fig. 4*F*). Sildenafil did not significantly delay the time from addition of the drug to onset of contractions; rather, a prompt reaction was seen (Fig. 4*G*).

DISCUSSION

In the present study, we combined structural and functional imaging of intact prostate tissue to characterize SMC compartments and their function within the prostate. Our approach using isolated prostate glands and ducts largely maintains tissue architecture and allows assessment of pharmacologic effects. It is therefore suitable for systematic testing of drugs assumed to affect prostate function or

also visible (*). *J–L*) PDE5 in SMCs of a big human prostate duct (d). It shows several layers of SMCs (+) that express SMA and PDE5, as confirmed in the merged image. Dotted lines: the lumen and epithelium of the duct directly surrounded by SMCs (+). *M*) Smaller human prostate duct. DAPI staining shows a longitudinal section of a prostate duct (d). Dotted lines: the diameter (lumen and epithelium). Inset: colocalization of SMA and PDE5 in the SMCs surrounding the epithelium. Scale bars: (*A*) 1 mm; (*B*) 100 μm; (*C–E*) 75 μm; (*F, G*) 200 μm; (H–I) 25 μm; (*J–M*) 50 μm.

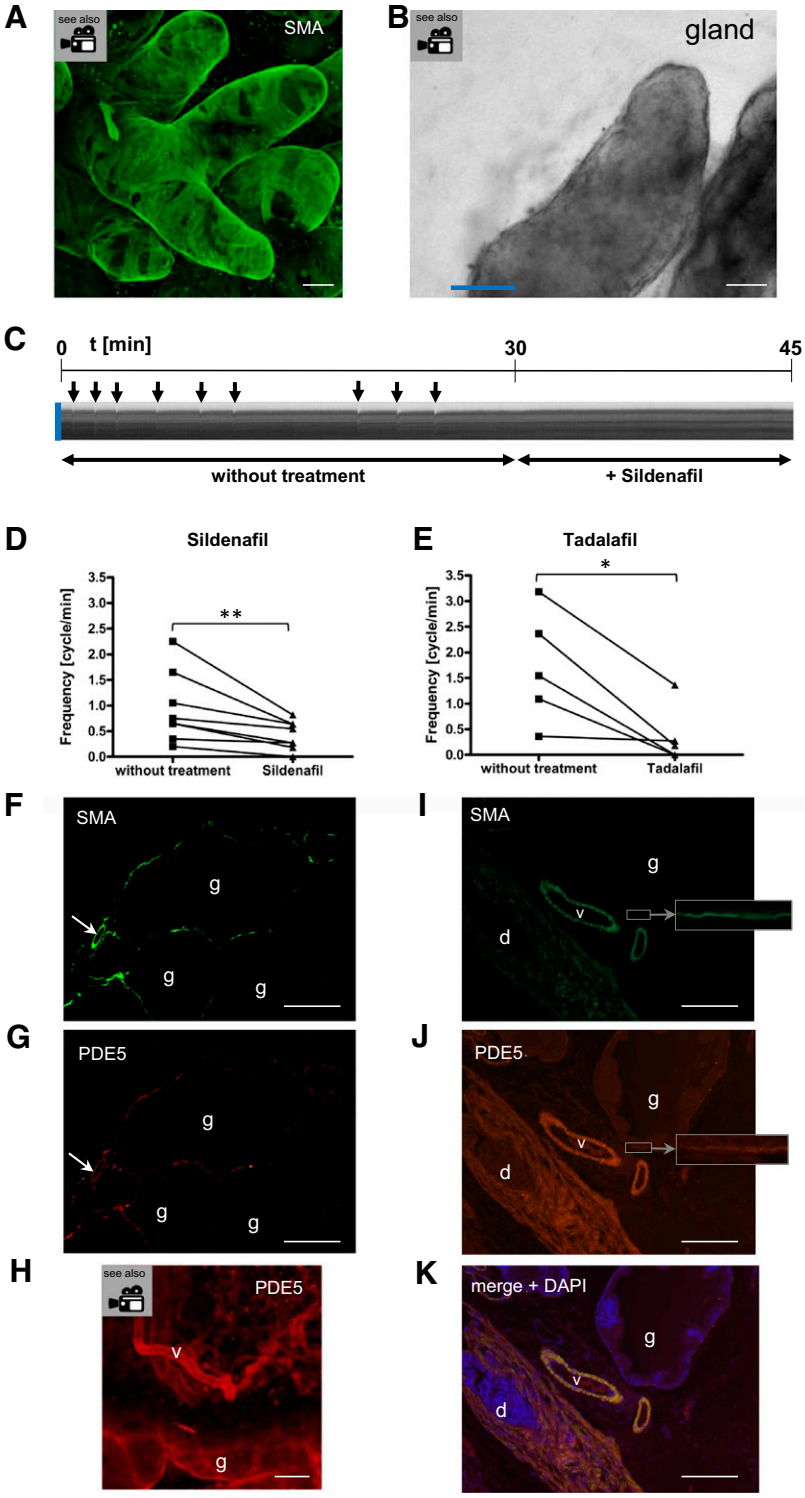

Figure 3. Visualization of contractile pattern in rat prostate gland and PDE5 localization in glandular, vascular, and ductal SMCs. *A*) Frame shot from Supplemental Movie 4 shows SMCs (SMA^+) surrounding rat prostate glands. Visualization by the 3-dimensional CLARITY approach allows appreciation of a tight association of SMCs around the prostate glands. (See Supplemental Movie 4 for 3-dimensional view.) *B*) Frame shot from Supplemental Movie 5 shows a transilluminated view of an isolated prostate gland used for time-lapse imaging. The line at the left lower margin indicates the position of the virtual slice that is followed over time in *C*. Scale bars: (*A*, *B*) 100 μm. *C*) Time-lapse imaging at the position indicated in *B* as a blue line is followed through the time stack. Contractions are visible as twitches (arrows). Spontaneous contractions occur in a slightly irregular pattern. Sildenafil reduced (or, in this example, abolished) contractile frequency. *D*) Sildenafil significantly reduced contractile frequency in rat prostate glands ($n = 8$) $^{**}P < 0.01$. *E*) Comparable results were visible with tadalafil ($n = 5$). $^{*}P < 0.05$. *F*, *G*) SMA and PDE5 immunostaining showed corresponding localizations in periglandular (g) SMCs. A positive vessel was also visible (arrow). *H*) Frame shot of PDE5 expression detected by the CLARITY approach. PDE5 expression is localized to glands (g) and along vessels (v) of the rat. Also refer to Supplemental Movie 6 for 3-dimensional appreciation. Scale bar, 75 μm. *I*–*K*) Double staining of SMA and PDE5 in gland (g), vessel (v), and duct (d) shows colocalization in all contractile cells (merged image). Insets: enlargements of the periglandular muscle layer. Nuclear counterstain: DAPI. Scale bars, 50 μm.

the prostatic component of the emission phase of ejaculation. Beside the vessels, we discriminated distinct SMC compartments in glands and ducts with different spatial architecture, function, and pharmacologic response to PDE5 inhibition. In prostate ducts which were characterized by high amounts of PDE5-expressing SMCs we directly uncovered the absence of spontaneous contractions and ensuing lack of sildenafil effects. Interestingly, data also showed that noradrenaline-induced contractions of prostatic ducts, as found during ejaculation, remain unaltered in the presence of sildenafil treatment.

Prostate ducts lacked spontaneous contractions, whereas isolated prostate glands exhibited spontaneous contractile activity. These contractions may provide a basal muscular tone and could be important for agitation of secretions in the glandular lumen. This finding supports the idea of pacemaker cells which generate contractile activity, suggested in human and guinea pig

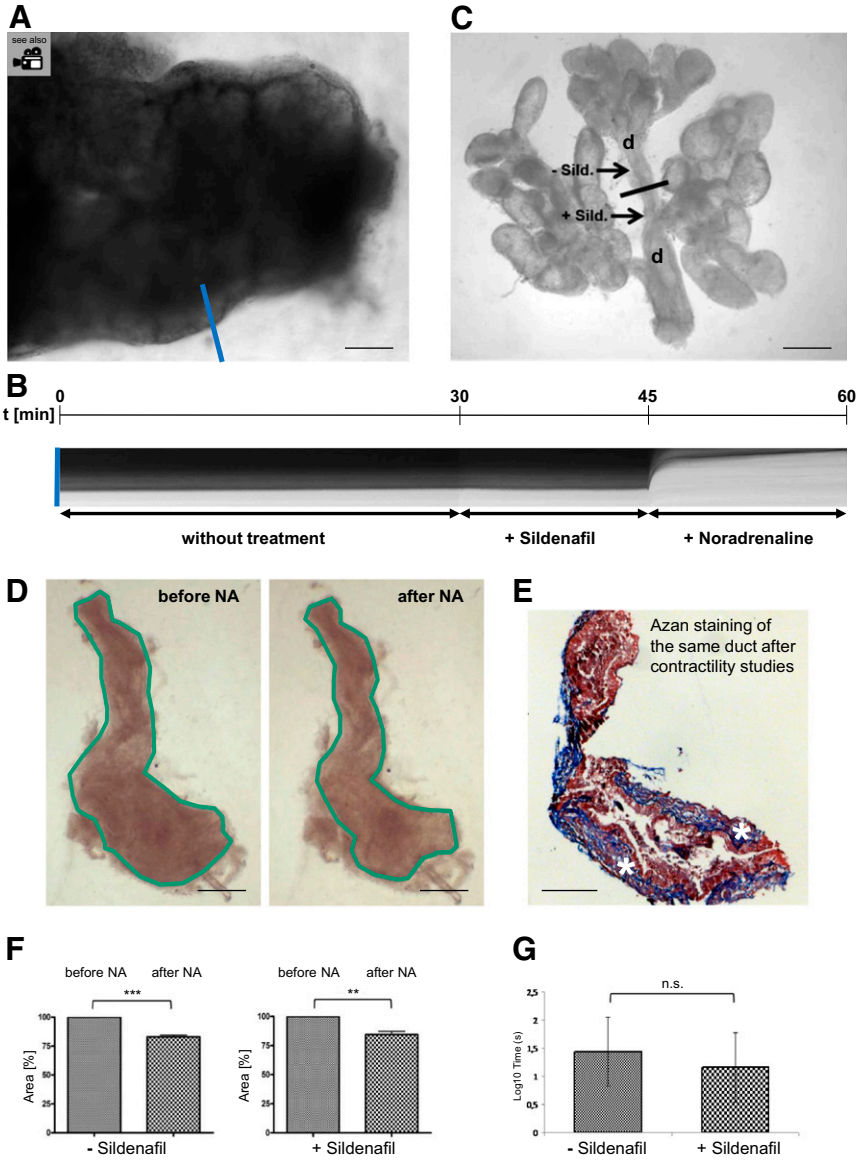

Figure 4. Prostate duct shows absence of spontaneous contractions and no sildenafil effects on noradrenaline-induced contractions. *A*) Frame shot from Supplemental Movie 7 shows the transillumination image of an isolated duct and the position of the virtual section being followed over time (*B*). Scale bar, 75 μm. *B*) Absence of twitches illustrates missing spontaneous activity and no sildenafil effect. When noradrenaline is added, the contraction is large and therefore appears as a sharp peak. Scale bar, 200 μm. *C*) Illustration of the procedure used to assess potential effects of sildenafil pretreatment on noradrenaline-induced duct contractions. Ducts (d) were cut in two parts and exposed to either sildenafil (+Sild.) or vehicle (−Sild.). *D*) Transillumination images of a prostate duct before and after the addition of noradrenaline illustrate area reduction as a means to assess and quantify the contraction. Scale bar, 100 μm. *E*) Corresponding azan staining of the material used in *D* confirms that visualization was performed in a duct portion of prostate tissue. Asterisks: characteristic smooth muscle layers of the duct. Scale bar, 150 μm. *F*) Contraction after the addition of noradrenaline occurred irrespective of sildenafil pretreatment. Area before addition of noradrenaline was set as 100%. $^{**}P < 0.01$; $^{***}P < 0.005$. *G*) No significant difference (n.s.) was found in the time delay from addition of noradrenaline to the beginning of the contraction.

prostate cells, independent of neuronal activation (31). Because noradrenaline effects on glandular acini were relatively weak, contractions of the secretory system (glands) may be of limited importance in the context of ejaculation physiology, different from the transport system (excretory ducts). Periglandular SMCs were shown to express PDE5, and the addition of sildenafil or tadalafil resulted in diminished contractile frequency. It would be interesting to know whether long-term treatment with PDE5 inhibitors results in an increasing number of prostatic concretions, caused by reduced agitation of secretions. Currently, long-term experience with PDE5 inhibitors in men with LUTS is limited to one trial with tadalafil with only a 1 yr follow-up (32).

Because of the different architecture of interstitial SMCs in the prostate, functionally intact glands can be isolated only in rodents. Intact human tissue pieces and isolated rat glands showed spontaneous contractility in a slightly irregular pattern at a similar range of frequencies, and reactions to drugs like sildenafil and noradrenaline are comparable. Our data suggest that in human stromal tissue (with its high amounts of SMCs around glandular structures), the physiologic role of spontaneous contractions may also be associated with glandular function.

Prostate ducts may be seen as a conduit serving to expel secretions during ejaculation which is highlighted by our finding of powerful contractions observed upon noradrenaline exposure, whereas in unstimulated conditions, no spontaneous contractile activity was detected. To our knowledge, this study is the first to investigate the effects of a PDE5 inhibitor on prostate ducts. PDE5 inhibitors did not affect noradrenaline-induced contractions that mediate ejaculation. Thus, PDE5 inhibitor-induced disturbances of prostate secretion during ejaculation are unlikely. This finding is of clinical relevance, given that drugs alternatively used for the treatment of BPH such as α_1-adrenergic blockers are known to negatively affect ejaculation (24, 25). Whereas α_1-adrenergic receptor inhibitors and ejaculation-mediating noradrenaline bind to the same membrane receptor (33), PDE5 inhibitors do not;

they inhibit hydrolysis of intracellular cGMP by PDE5 (34). The insensitivity to PDE5 inhibitors in the ducts cannot be explained by missing PDE5 in these structures, as PDE5 was readily detected in SMCs of prostate ducts from both human and rat. However, the precise role of PDE5 in prostate ducts is not clear. It is plausible that (basal) PDE5 activity limits cGMP levels and thus reduces SMC relaxation. Thereby a basic tension of the duct musculature may be maintained to ensure the rapid catecholamine-induced contractions that are necessary for ejaculation.

In comparison to sole analyses of ejaculation and ejaculate, our data give much more information about the physiology of the prostatic component of ejaculation. Different from organ bath studies with strips of the whole prostate (14, 21–23), our methodology allows discrimination between effects on SMCs of the ducts and the interstitial periglandular compartment.

The CLARITY approach (28, 30) added the third dimension to the usual histologic techniques and valuable information to our understanding of the spatial arrangement and function of SMCs around the prostate glands. In human prostate, SMCs not only surrounded the epithelial layer of the glands, but were detectable in all parts of the interstitial compartment with different orientation. In the rat, the 3-dimensional projection of the SMCs showed a bandage-like arrangement around the glands, with regions devoid of SMCs consistent with the observation of "patchy" contractile activity in our functional studies.

Besides PDE5 [see Gacci *et al.* (20)], other components of cGMP pathways now represent potential targets for therapeutic intervention. These include other PDEs (35), as well as cGMP-generating guanylyl cyclases (23, 36, 37). In all cases, the beneficial cGMP effect for patients with BPH may be the reduction of muscular tone in the pathologically enlarged interstitial compartment, along with the maintenance of the noradrenaline-induced contractile function in the ducts.

In summary, our study advances our understanding of different SMC compartments in the prostate with respect to their distinct spatial arrangement, physiologic function, and pharmacologic responses. FJ

ACKNOWLEDGMENTS

The authors thank Dr. Laurinda Jaffe (University of Connecticut Health Center, Farmington, CT), for providing us with anti-PDE5 antibodies; Dr. Dieter Müller (Justus-Liebig-University Giessen, Germany), for helpful discussions; and Ingrid Schneider-Hüther, Tania Bloch, and Kerstin Wilhelm (Justus-Liebig-University), for excellent technical assistance. Funding was provided by the Deutsche Forschungsgemeinschaft Grant GRK 1871 and funding from Monash University, Australia, to the International Research Training Group (IRTG), a collaboration between Justus-Liebig-University Giessen and Monash University. The authors declare no conflicts of interest.

AUTHOR CONTRIBUTIONS

R. Kügler, M. Seidensticker, and S. Tasch performed the experiments; A. Kaschtanow and C. U. Tomczyk performed the CLARITY imaging; R. Kügler, A. Mietens, M. Seidensticker, and D. Beyer contributed to the statistical analyses; F. M. Wagenlehner provided material support; F. M. Wagenlehner, Y. Tjahjono, G. P. Risbridger, B. Exintaris, and S. Ellem contributed valuable advice to the redaction of the manuscript; R. Kügler, A. Mietens, and R. Middendorff wrote the manuscript; and R. Middendorff designed the study and directed the project.

REFERENCES

1. Roehrborn, C. G. (2008) Pathology of benign prostatic hyperplasia. *Int. J. Impot. Res.* **20**(Suppl 3), S11–S18
2. Ichihara, I., Kallio, M., and Pelliniemi, L. J. (1978) Light and electron microscopy of the ducts and their subepithelial tissue in the rat ventral prostate. *Cell Tissue Res.* **192**, 381–390
3. Lee, C., Sensibar, J. A., Dudek, S. M., Hiipakka, R. A., and Liao, S. T. (1990) Prostatic ductal system in rats: regional variation in morphological and functional activities. *Biol. Reprod.* **43**, 1079–1086
4. Nemeth, J. A., and Lee, C. (1996) Prostatic ductal system in rats: regional variation in stromal organization. *Prostate* **28**, 124–128
5. Plant, T. M., and Zeleznik, A. J. (2015) *Knobil and Neill's Physiology of Reproduction*, Elsevier Science, Burlington, MA, USA
6. McNeal, J. E. (1983) *The Prostate Gland, Morphology and Pathobiology*, Burroughs Wellcome Company, Princeton, NJ, USA
7. AUA Practice Guidelines Committee (2003) AUA guideline on management of benign prostatic hyperplasia (2003). Chapter 1: diagnosis and treatment recommendations. *J. Urol.* **170**, 530–547
8. McVary, K. T., Roehrborn, C. G., Avins, A. L., Barry, M. J., Bruskewitz, R. C., Donnell, R. F., Foster, H. E., Jr., Gonzalez, C. M., Kaplan, S. A., Penson, D. F., Ulchaker, J. C., and Wei, J. T. (2011) Update on AUA guideline on the management of benign prostatic hyperplasia. *J. Urol.* **185**, 1793–1803
9. Bozkurt, O., Demir, O., Sen, V., and Esen, A. (2015) Silodosin causes impaired ejaculation and enlargement of seminal vesicles in sexually active men treated for lower urinary tract symptoms suggestive of benign prostatic hyperplasia. *Urology* **85**, 1085–1089
10. Capogrosso, P., Serino, A., Ventimiglia, E., Boeri, L., Dehò, F., Damiano, R., Briganti, A., Montorsi, F., and Salonia, A. (2015) Effects of silodosin on sexual function: realistic picture from the everyday clinical practice. *Andrology* **3**, 1076–1081
11. Tatemichi, S., Kobayashi, K., Yokoi, R., Kobayashi, K., Maruyama, K., Hoyano, Y., Kobayashi, M., Kuroda, J., and Kusama, H. (2012) Comparison of the effects of four α1-adrenoceptor antagonists on ejaculatory function in rats. *Urology* **80**, 486.e9–486.e16
12. Wang, X.-H., Wang, X., Shi, M.-J., Li, S., Liu, T., and Zhang, X.-H. (2015) Systematic review and meta-analysis on phosphodiesterase 5 inhibitors and α-adrenoceptor antagonists used alone or combined for treatment of LUTS due to BPH. *Asian J. Androl.* **17**, 1022–1032
13. Oelke, M., Bachmann, A., Descazeaud, A., Emberton, M., Gravas, S., Michel, M. C., N'dow, J., Nordling, J., and de la Rosette, J. J.; European Association of Urology. (2013) EAU guidelines on the treatment and follow-up of non-neurogenic male lower urinary tract symptoms including benign prostatic obstruction. *Eur. Urol.* **64**, 118–140
14. Ückert, S., Küthe, A., Jonas, U., and Stief, C. G. (2001) Characterization and functional relevance of cyclic nucleotide phosphodiesterase isoenzymes of the human prostate. *J. Urol.* **166**, 2484–2490
15. Gacci, M., Corona, G., Salvi, M., Vignozzi, L., McVary, K. T., Kaplan, S. A., Roehrborn, C. G., Serni, S., Mirone, V., Carini, M., and Maggi, M. (2012) A systematic review and meta-analysis on the use of phosphodiesterase 5 inhibitors alone or in combination with α-blockers for lower urinary tract symptoms due to benign prostatic hyperplasia. *Eur. Urol.* **61**, 994–1003
16. Wang, X., Wang, X., Li, S., Meng, Z., Liu, T., and Zhang, X. (2014) Comparative effectiveness of oral drug therapies for lower urinary tract symptoms due to benign prostatic hyperplasia: a systematic review and network meta-analysis. *PLoS One* **9**, e107593

17. Fibbi, B., Morelli, A., Vignozzi, L., Filippi, S., Chavalmane, A., De Vita, G., Marini, M., Gacci, M., Vannelli, G. B., Sandner, P., and Maggi, M. (2010) Characterization of phosphodiesterase type 5 expression and functional activity in the human male lower urinary tract. *J. Sex. Med.* **7**, 59–69
18. Rybalkin, S. D., Rybalkina, I. G., Feil, R., Hofmann, F., and Beavo, J. A. (2002) Regulation of cGMP-specific phosphodiesterase (PDE5) phosphorylation in smooth muscle cells. *J. Biol. Chem.* **277**, 3310–3317
19. Juilfs, D. M., Soderling, S., Burns, F., and Beavo, J. A. (1999) Cyclic GMP as substrate and regulator of cyclic nucleotide phosphodiesterases (PDEs). *Rev. Physiol. Biochem. Pharmacol.* **135**, 67–104
20. Gacci, M., Andersson, K.-E., Chapple, C., Maggi, M., Mirone, V., Oelke, M., Porst, H., Roehrborn, C., Stief, C., and Giuliano, F. (2016) Latest evidence on the use of phosphodiesterase type 5 inhibitors for the treatment of lower urinary tract symptoms secondary to benign prostatic hyperplasia. *Eur. Urol.* **70**, 124–133
21. Ückert, S., Sormes, M., Kedia, G., Scheller, F., Knapp, W. H., Jonas, U., and Stief, C. G. (2008) Effects of phosphodiesterase inhibitors on tension induced by norepinephrine and accumulation of cyclic nucleotides in isolated human prostatic tissue. *Urology* **71**, 526–530
22. Angulo, J., Cuevas, P., Fernández, A., La Fuente, J. M., Allona, A., Moncada, I., and Sáenz de Tejada, I. (2012) Tadalafil enhances the inhibitory effects of tamsulosin on neurogenic contractions of human prostate and bladder neck. *J. Sex. Med.* **9**, 2293–2306
23. Dey, A., Lang, R. J., and Exintaris, B. (2012) Nitric oxide signaling pathways involved in the inhibition of spontaneous activity in the guinea pig prostate. *J. Urol.* **187**, 2254–2260
24. Chapple, C. R. (2004) Pharmacological therapy of benign prostatic hyperplasia/lower urinary tract symptoms: an overview for the practising clinician. *BJU Int.* **94**, 738–744
25. Kaplan, S. A. (2009) Side effects of alpha-blocker use: retrograde ejaculation. *Rev. Urol.* **11**(Suppl 1), S14–S18
26. Wang, L., Zhang, X., Wang, G., Visweswariah, S. S., Lin, G., Xin, Z., Lue, T. F., and Lin, C.-S. (2015) Lobe-specific expression of phosphodiesterase 5 in rat prostate. *Urology* **85**, 703.e7–703.e13
27. Mietens, A., Tasch, S., Stammler, A., Konrad, L., Feuerstacke, C., and Middendorff, R. (2014) Time-lapse imaging as a tool to investigate contractility of the epididymal duct: effects of cGMP signaling. *PLoS One* **9**, e92603
28. Chung, K., and Deisseroth, K. (2013) CLARITY for mapping the nervous system. *Nat. Methods* **10**, 508–513
29. Yang, B., Treweek, J. B., Kulkarni, R. P., Deverman, B. E., Chen, C.-K., Lubeck, E., Shah, S., Cai, L., and Gradinaru, V. (2014) Single-cell phenotyping within transparent intact tissue through whole-body clearing. *Cell* **158**, 945–958
30. Saboor, F., Reckmann, A. N., Tomczyk, C. U., Peters, D. M., Weissmann, N., Kaschtanow, A., Schermuly, R. T., Michurina, T. V., Enikolopov, G., Müller, D., Mietens, A., and Middendorff, R. (2016) Nestin-expressing vascular wall cells drive development of pulmonary hypertension. *Eur. Respir. J.* **47**, 876–888
31. Nguyen, D.-T. T., Dey, A., Lang, R. J., Ventura, S., and Exintaris, B. (2011) Contractility and pacemaker cells in the prostate gland. *J. Urol.* **185**, 347–351
32. Donatucci, C. F., Brock, G. B., Goldfischer, E. R., Pommerville, P. J., Elion-Mboussa, A., Kissel, J. D., and Viktrup, L. (2011) Tadalafil administered once daily for lower urinary tract symptoms secondary to benign prostatic hyperplasia: a 1-year, open-label extension study. *BJU Int.* **107**, 1110–1116
33. Andersson, K.-E., and Gratzke, C. (2007) Pharmacology of alpha1-adrenoceptor antagonists in the lower urinary tract and central nervous system. *Nat. Clin. Pract. Urol.* **4**, 368–378
34. Corbin, J. D., and Francis, S. H. (1999) Cyclic GMP phosphodiesterase-5: target of sildenafil. *J. Biol. Chem.* **274**, 13729–13732
35. Hennenberg, M., Schott, M., Kan, A., Keller, P., Tamalunas, A., Ciotkowska, A., Rutz, B., Wang, Y., Strittmatter, F., Herlemann, A., Yu, Q., Stief, C. G., and Gratzke, C. (2016) Inhibition of adrenergic and non-adrenergic smooth muscle contraction in the human prostate by the phosphodiesterase 10-selective inhibitor TC-E 5005. *Prostate* **76**, 1364–1374
36. Müller, D., Mukhopadhyay, A. K., Davidoff, M. S., and Middendorff, R. (2011) Cyclic GMP signaling in rat urinary bladder, prostate, and epididymis: tissue-specific changes with aging and in response to Leydig cell depletion. *Reproduction* **142**, 333–343
37. Calmasini, F. B., Alexandre, E. C., Silva, F. H., De Nucci, G., Antunes, E., D'Ancona, C. A., and Mónica, F. Z. (2016) Soluble guanylate cyclase modulators, BAY 41-2272 and BAY 60-2770, inhibit human and rabbit prostate contractility. *Urology* **94**, 312.e9–312.e15

Received for publication June 18, 2017.
Accepted for publication October 16, 2017.